Analysis of DNA−Protamine Interactions by Optical Detection of Magnetic Resonance†

Maria C. Prieto,‡,§ August H. Maki,*,‡ and Rod Balhorn‖

Chemistry Department, University of California, Davis, California 95616, and Biology and Biotechnology Research, Lawrence Livermore National Laboratory, Livermore, California 94550

Received May 7, 1997; Revised Manuscript Received July 17, 1997⊗

ABSTRACT: Optically detected magnetic resonance (ODMR) has been used to identify the binding site of a synthetic protamine subdomain to the major groove of DNA. A 14 amino acid peptide (R_6WGR_6) analog of the central DNA binding domain of bull protamine was synthesized with phenylalanine replaced by tryptophan (Trp). The peptide was bound to double-stranded poly(dABrdU) and to calf thymus DNA (CT DNA) and the complexes characterized as "wet" solids using ODMR techniques. The appearance of the $D + E$ transition in the slow passage ODMR and of short-lived components in the phosphorescence decay of the complex of R_6WGR_6 with poly(dABrdU) is diagnostic of a heavy atom effect. This can only occur if the peptide binds in the major groove of poly(dABrdU). The microenvironment of Trp in the nucleoprotein complex was characterized by phosphorescence, radiative decay lifetimes, and low-temperature ODMR measurements before and after binding to DNA. Bathochromic shifts in the phosphorescence emission upon exciting to the red in CT DNA−peptide suggest that the Trp is in a polar environment, while the red-shifted position of the 0,0-band emission points to a more polarizable environment. The heavy atom effect strongly suggests a Trp location within the major groove of DNA. A partial stacking of Trp with the polarizable nucleobases and simultaneous interactions with the phosphate-guanidinium ion pairs and/or water molecules in the major groove of DNA which might not be totally displaced upon binding of the peptide could explain this conflicting evidence. Extrapolation of results from the system studied to protamine binding in sperm chromatin strongly suggests that the predominant binding site of protamine is the major groove of DNA.

Protamine binding to DNA produces a highly condensed form of chromatin within the sperm cell nucleus and inactivates the sperm genome (*1*). Protamine synthesis occurs during late spermiogenesis (*2*), coincident with the elongation of the spermatid nucleus and the final stage of DNA compaction. Protamine is an arginine-rich protein that displaces histones and transition proteins in mammalian sperm cells. The nucleosome packaging of DNA from somatic cells therefore is eliminated. Bull protamine is a 50 amino acid peptide representing a class of highly conserved proteins known as protamine 1. The bull protamine sequence is ARYRCCLTH[10]SGSRCRRRRR[20]RRC-RRRRRRF[30]GRRRRRRVCC[40]RRYTVIRCTR[50]Q. It consists of three domains: the central region with three strings of several arginines (R)[1] each (the DNA binding domain), the amino terminal region, and the carboxy terminal end. Hydrogens in the positively charged guanidinium groups of protamine interact electrostatically with the phosphate groups of DNA, and a biochemically inert precipitate forms upon its binding to DNA. This charge neutralization by protamine yields the most condensed form of DNA packaging known in eukaryotic cells, about 40-fold greater than that in somatic cell nuclei (*3*).

The insolubility of the DNA−protamine complex has rendered it useless for structure characterization by techniques like solution NMR and spectrophotometry. Until recently, X-ray diffraction has been the main technique applied to the study of DNA−protamine interactions, even though attempts to crystallize the DNA−protamine complex have not been successful. Early X-ray diffraction studies suggested minor groove binding (*4*) while other studies of chemical reactivity, Raman spectra, and X-ray diffraction of DNA complexed with small arginine-containing oligopeptides, indicated major groove binding. In complexes with basic peptides, DNA was found to retain a β-DNA helix conformation regardless of water content (*4*, *5*). An α-helix conformation was found for protamine in a protamine−tRNA single crystal (*4*, *6*). This was disputed by Balhorn (*7*) using a previous infrared study (*8*) and modeling with distance arguments. Another conflicting piece of information was provided by fiber diffraction on dry-spun fibers of nucleoprotamine and computer modeling of a polyhexapeptide−DNA complex (*4*). This work found the protein residues

† This research was performed in part at the Lawrence Livermore National Laboratory under the auspices of the U.S. Department of Energy and supported by Contract W-7405-ENG-48 and at the University of California, Davis, with support by NIH Grant ES-02662.

* Author to whom correspondence should be addressed.

‡ University of California, Davis.

§ Present address: Analytical Science Division, Lawrence Livermore National Laboratory, Livermore, CA 94550.

‖ Lawrence Livermore National Laboratory.

⊗ Abstract published in *Advance ACS Abstracts,* September 15, 1997.

[1] Abbreviations: BrdU, 5-bromodeoxyuridylic acid; CT DNA, calf-thymus deoxyribonucleic acid; EG, ethylene glycol; F and Phe, phenylalanine; G, glycine; HAE, heavy atom effect; Lys-Trp-Lys, lysyl tryptophanyl lysine; MIDP, microwave-induced delayed phosphorescence; NMR, nuclear magnetic resonance; ODMR, optically detected magnetic resonance; poly(dABrdU), double helix formed by two strands of the alternating dA, BrdU DNA polymer; R, arginine; SLR, spin-lattice relaxation; TRIS, tris(hydroxymethyl)aminomethane; Trp and W, tryptophan; Tyr, tyrosine; zfs, zero field splittings.

S0006-2960(97)01061-1 CCC: $14.00

mainly in the β conformation and protamine bound in the major groove of DNA. They also suggest that neutral peptide residues in compact nucleoprotamine could interact with the minor grooves of other complexes, allowing very little water to remain in the grooves.

Recent Raman studies on DNA−salmine (salmon protamine) complexes have provided evidence for a novel secondary structure attained by bound protamine and verified a modified β-form for DNA in the complex (*9*). The model adopted included major groove binding, which was supported by computer modeling studies with energy minimization (*10*). Intercalators like actinomycin D were found to bind readily to DNA in somatic nuclei, while they did not bind as readily to spermatid or DNA in mature sperm (*11*, *12*). Benzo[*a*]-pyrene, a minor groove binder, will not alkylate sperm DNA, suggesting that protamine physically blocks it (*12*, *13*). Both results were interpreted as an indication that protamine occupies the minor groove of DNA directly. However, interlocking of the phosphate groups on the two phosphodiester chains by protamine bound in the major groove would not allow actinomycin D to intercalate in DNA; the bases must unstack to permit intercalation, forcing the phosphate groups on the two strands to move in opposite directions away from each other (*4*). By cross-linking together the two phosphodiester chains, protamine binding would inhibit such a shift. The minor groove could also be rendered unavailable for binding when DNA−protamine aggregates are formed by stacking of complexes against the minor grooves (*7*).

Optical detection of magnetic resonance (ODMR) examines the triplet state of an aromatic chromophore while monitoring, in the work to be presented here, its phosphorescence. This technique senses changes in polarity and polarizability in the surrounding microenvironment of the chromophore. Heavy atoms in the vicinity of a chromophore (at approximately van der Waals distances) provide an indicator of short-range interactions. The external heavy atom effect (HAE) depends both on distance and location of the perturbing heavy atom with respect to the molecular axes of the chromophore. The main purpose of this study is to identify the binding site of protamine and determine whether it binds to the minor or major groove of DNA. A portion of the central binding domain (R_6FGR_6, underlined in the sequence given above) was synthesized, with Phe replaced by Trp. The 14 amino acid peptide was then bound to double-stranded poly(dABrdU). Replacing thymine with 5-bromouracil in a DNA helix places the bromine atom in the major groove of DNA. The observation of a HAE (*14*) induced by the bromine atom on Trp would require the peptide to bind in or slightly above the major groove of DNA in order for Trp to achieve van der Waals contact with the heavy atom, a requirement for the external HAE (*15*−*19*). Van der Waals contact with a heavy atom such as Br greatly reduces individual triplet state sublevel lifetimes, induces radiative decay in otherwise radiationless sublevels, induces fluorescence quenching due to enhanced intersystem crossing, and enhances the Trp phosphorescence yield (*16*, *20*, *21*). Reduced sublevel lifetimes allow slow passage ODMR experiments to be conducted at a faster microwave sweep rate, discriminating in favor of the perturbed Trp (*22*). This approach was used to demonstrate that the model peptide employed in this work, and thus bull protamine by inference, binds to the major groove of DNA.

MATERIALS AND METHODS

Sample Preparation. R_6WGR_6 was synthesized using an automated peptide synthesizer and the fluorenylmethoxycarbonyl (FMOC) protection method, and the crude peptide was subsequently purified by HPLC. Batches of peptide were synthesized either at the Protein Structure Laboratory, University of California, Davis, CA, or at the Biology and Biotechnology Research Program at Lawrence Livermore National Laboratory (LLNL), Livermore, CA. CT DNA was purchased from Sigma Chemical Co., St. Louis, MO. Samples were dissolved in TRIS buffer (10 mM, pH 7) with ethylene glycol (20−25%, v/v) as cryosolvent. The peptide concentration ranged from 0.3 to 0.5 mM. Poly(dABrdU) (Biogenetics Research Corp., Chardon, OH) was dissolved in 10 mM pH 7 TRIS buffer to a concentration of 4 mM in PO_4 and stored at 0 °C. The high complementarity of the sequence and its melting profile assured us that the synthetic oligonucleotide remained in a double-stranded form. The 17 base pair duplex, oligo(dABrdU), was synthesized using an Applied Biosystems Synthesizer (ABS, Inc., Foster City, CA), following established protocols as they appear in their Procedures Manual. The DNA oligomer was synthesized at the Biology and Biotechnology Research Program, Lawrence Livermore National Laboratory (LLNL), Livermore, CA. Complex binding was carried out directly in 2 mm i.d. Suprasil tubes, each of 35−40 μL volume. Three different types of complexes were prepared: R_6WGR_6/CT DNA, R_6WGR_6/Poly(dABrdU), and R_6WGR_6/oligo(dABrdU). All DNA−protamine complexes were studied as wet solids. Three procedures were used to prepare the peptide−CT DNA complexes: (1) mixing of unsonicated CT DNA and peptide, (2) mixing of sonicated CT DNA with peptide under the same conditions as 1, and (3) sonicated CT DNA and peptide each dissolved in 1 M NaCl and 10 mM TRIS buffer were mixed and dialyzed (MW 500; Spectrum Medical Industries, Los Angeles, CA; only buffer is permeable at this pore size) at ∼4 °C against three exchanges of salt-free 10 mM TRIS buffer. No precipitate forms when peptide and DNA are mixed initially in 1 M NaCl; a very fine precipitate results from this method after dialysis. The precipitate was recovered by centrifugation after cooling to ∼4 °C. Sonication of the DNA stock solution used in methods 2 and 3 was carried out in five steps using a Heat Systems-Ultrasonics, Inc., Model W-220 sonicator equipped with a microtip, cooling the solution in ice between steps. The size of unsonicated DNA is (25−30) × 10^6 Da, ca. 45 500 base pairs; sonicated DNA is approximately (5−10) × 10^6 Da or ca. 7600 bp long. All samples were prepared using a 12/1 ratio of phosphate to Trp, since the peptide contains 12 Arg and 1 Trp and each of the Arg binds to a phosphate group. Complexes with brominated DNAs were prepared by mixing the peptide and nucleotide solutions directly in a Suprasil tube, discarding the supernatant solution, and repeating this procedure until enough precipitated sample was obtained. The mixing ratio was 12/1 phosphate to peptide, as in the other cases. All precipitated complexes were treated similarly. The precipitate was centrifuged and the supernant was discarded. The final step involved rinsing the precipitate with buffer that contained ∼23% (v/v) ethylene glycol, which reduced the amount of unbound peptide. The initial presence of unbound peptide was more evident when the samples with brominated DNA were prepared. The relative amounts

of unperturbed vs perturbed Trp could be estimated from the phosphorescence decay profile.

Phosphorescence and ODMR Spectroscopic Methods. Descriptions of the ODMR technique used in this study (*23*−*25*) and the instrumental set up employed (*25*) have been published. Phosphorescence spectra and decay kinetics were measured at three temperatures: 77, 4.2, and 1.2 K. Excitation was performed at 295 nm (16 nm band-pass and 3 nm emission band-pass), except when noted. The cycle time for kinetic measurements on unperturbed Trp was 65 s, with 33 s used for excitation, and for perturbed Trp it was 6 s, with 3 s used for excitation. All decays were deconvoluted by a nonlinear least-squares Marquardt algorithm designed to minimize the ψ-square of the fitting function and whose goodness-of-fit was monitored via a residuals plot. Experiments in which the origin of the phosphorescence spectrum is monitored as a function of the wavelength of excitation were used to determine whether a Trp is buried or solvent exposed (*26*). Tryptophan exposed to a polar environment typically exhibits a larger dependence on the excitation wavelength than Trp residues in nonpolar but polarizable environments (*26*). These experiments were compared with results obtained for L-Trp in a polar solvent medium.

ODMR and microwave-induced delayed phosphorescence (MIDP) (*27*) measurements were conducted at 1.2 K, where spin-lattice relaxation is slow relative to the individual triplet sublevel decays, and the sublevels attain characteristic populations largely through intersystem crossing and decay processes. In slow passage ODMR, the sample is irradiated with variable frequency microwave energy under continuous optical pumping. Only a sublevel that is coupled to a radiative sublevel (*i.e.*, T_x in unperturbed Trp) and whose population differs therefrom, is detectable optically at resonance. Microwave sweep rates for unperturbed Trp were on the order of 50 MHz/s, while for perturbed Trp they were on the order of 3 GHz/s. The decay rates of the individual sublevels were obtained by either MIDP or the fast passage transient experiment (*28*). MIDP gives the decay constants of the long-lived nonradiative sublevels, while the fast passage was used to provide the decay constants for the radiative sublevels (mostly k_x in trp). k_x was also obtained by data manipulation of the MIDP response. In this technique, a phosphorescence decay is subtracted from the MIDP decay; the remaining response corresponds mainly to the radiative sublevel, k_x.

RESULTS

Trp is the chromophore of choice for phosphorescence studies in proteins due to its lower S_1 and T_1 energy states (*25*). This was the reason we used a synthetic peptide in this study and substituted Trp for Phe in the binding region of protamine. Although the fluorescence of Trp is quenched by nucleic acid binding at ambient temperatures, its phosphorescence in nucleic acid complexes is readily observed in rigid media at low temperature (*25*). Phe and Tyr are not viable options as an optical probe since their entire luminescence is quenched by nucleic acid binding at all temperatures.

Phosphorescence and Triplet Lifetimes. Figure 1 shows the phosphorescence spectra of R_6WGR_6 (d and e) and four types of complexes (a−c and f) at 4.2 K. The wavelength of the phosphorescence 0,0-band peaks and the triplet

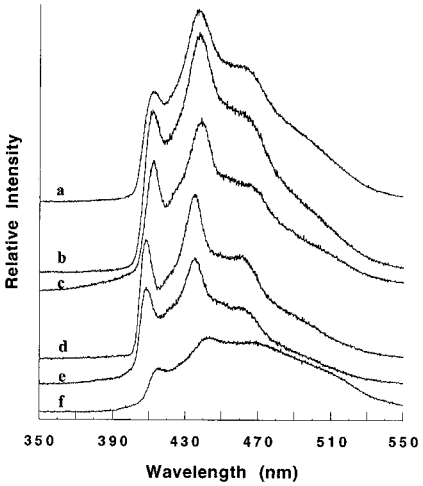

FIGURE 1: Phosphorescence spectra at 4.2 K of the peptide and peptide complexed to DNA under different binding conditions. (a) unsonicated CT DNA−peptide, (b) sonicated CT DNA−peptide, (c) CT DNA−peptide dialysis method (see text), (d) peptide in 10 mM TRIS, pH 7, containing 23% EG (v/v), (e) peptide at pH 13 in water/EG (23%), (f) poly(dABrdU)−peptide. All complexes are "wet" solids; excitation is at 295 nm.

lifetimes are given in Table 1. These parameters varied slightly among samples and from day to day. The peptide 0,0-band is red shifted by ca. 2.5 nm from that of L-Trp in solution. Complexes with CT DNA have red-shifted 0,0-bands relative to the peptide, the shift for the complex with sonicated DNA is 3.9 nm. The resolution and position of the 0,0-band maxima were independent of temperature in the peptide while the spectra of complexes were more poorly resolved at 77 K than at lower temperatures. The average width of the 0,0-band (full-width at half-height, FWHH) for the peptide at pH 7 was 11.4 ± 0.7 nm, while the complexes had broader 0,0-bands (Table 1). The complex formed with unsonicated DNA displays the broadest 0,0-band (26.1 ± 3 nm, data not shown) among the CT DNA complexes, while the narrowest occurs in the complex prepared by dialysis (12.1 ± 2 nm); the line width of the complex prepared using sonicated DNA is intermediate between these (17.8 ± 2 nm). The peptide phosphorescence decay at 4.2 K was fitted to a biexponential resulting in a major contribution attributed to Trp whose lifetime varied from 6.5 s (89%) to 6.8 s (95%) (Figure 2a, Table 1). The phosphorescence of the complex formed with sonicated DNA when fitted to a biexponential decay results in lifetimes of 6.1 s (67%) and 2.8 s (22%) at 4.2 K. The major component is attributed to a relatively unperturbed Trp (Figure 2b, Table 1). A portion of the minor 2.8 s component may originate from residual solvent in contact with the wet solid since a weak phosphorescence component of similar lifetime is found in TRIS/EG, as well as in L-tryptophan, the peptide, and CT DNA dissolved in this solvent. The intensity of this 2.4−3.3 s component (22−29% of the total phosphorescence in the peptide complexes with CT DNA) is estimated to be at least an order of magnitude too intense to originate from residual solvent. We suggest that a new somewhat perturbed Trp population with a shorter phosphorescence lifetime is present, representing Trp residues forced into a unique environment by binding to DNA. The only nucleobase that decays with a lifetime near 2.4 s is adenine. However, adenine can be excited only near 270 nm and emits to the blue of Trp. No such emission is observed (Figure 1, panels a−c). Furthermore, duplex CT

Table 1: Phosphorescence Lifetimes and Triplet Sublevel Decay Rates of Tryptophan in Various Environments

sample[a]	λ_{em} (nm)[b]	τ (s)[c]	k_x (s^{-1})[d]	k_y (s^{-1})[d]	k_z (s^{-1})[d]
L-Trp[e]	406.0 (10.4)	6.6 (95%) 2.3 (5%)	0.31	0.10	0.00
peptide (pH = 7)	408.3−408.7[f] (11.4)	6.5−6.8 (89−95%)[f] 1.3−2.9 (11−5%)	0.35[g]	0.13	0.10
peptide (pH 13)	408.9 (12.3)	6.8 (79%) 3.0 (10%) 0.3 (11%)		NA[i]	
CT DNA/peptide (sonicated DNA, mixing method)	412.1 (17.8)	6.1 (67%) 2.8 (22%) 0.4 (11%)	0.96[g]	0.11	0.11
CT DNA/peptide (dialysis method)	412.1 (12.1)	5.7 (56%) 2.4 (29%) 0.5 (15%)		NA[i]	
Poly(dABrdU) + peptide (mixing method)	415.0 (19.3)	2.7 (23%) 0.25 (31%) 0.04 (46%)	174[h]	78	1.5

[a] Samples were excited at 295 nm; $T = 4.2$ K for phosphorescence and lifetime measurements. [b] Average line widths (FWHH in nm) of 0,0-band are in parentheses. [c] See text for cycle times of unperturbed vs perturbed Trp; mean weighted residual was ≤0.06 for all measurements. [d] The sublevel decay constants were determined using MIDP and rapid passage transient techniques. [e] Sublevel decay rate constants, corrected for SLR, are from ref 33; λ_{em} and τ are from this research. [f] Range in measurements reflects the variability observed for different samples. [g] Decay constant is extracted by analysis of the MIDP transient response. [h] Obtained from rapid passage transient analysis (*28*), uncorrected for excitation intensity. [i] NA, not applicable.

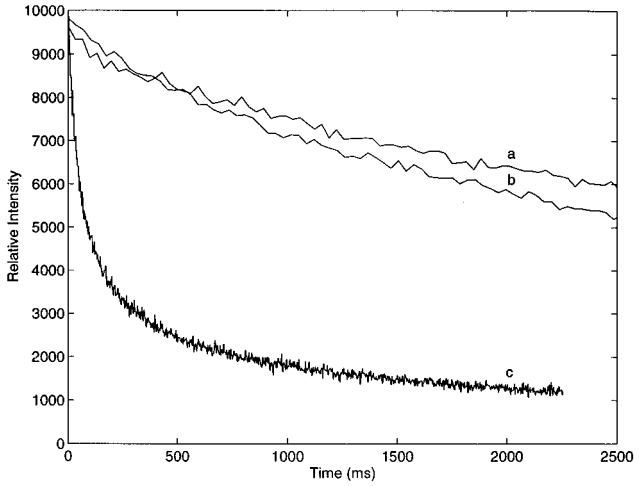

FIGURE 2: Phosphorescence decays at 4.2 K of the peptide and peptide complexed to DNA. (a) peptide, pH 7, (b) sonicated DNA−peptide complex; cycle time was 63 s (30 s excitation, 33 s emission in curves a and b) (c) Poly(dABrdU)−peptide complex; 6 s cycle time (3 s excitation, 3 s emission). Sample conditions are given in Figure 1 caption.

DNA phosphorescence has been shown to originate from thymine (*29*, *30*), which has a much shorter lifetime. CT DNA in our TRIS/EG buffer at 77 K decays with a major lifetime component of 0.23 s (90%) which we assign to thymine. A minor 2.45 s component (10%) is attributed to the solvent. Therefore, the relatively intense (22−29%) ∼2.4 s component observed in the peptide−CT DNA complex is reasonably assigned to a Trp population that decays more rapidly than does the unperturbed peptide.

Bathochromic Shifts. Table 2 shows the relationship between excitation wavelength and the 0,0-band peak wavelength. L-Trp in a polar solvent experiences a red shift (bathochromic shift) upon varying the excitation to a longer wavelength. Tryptophan in the peptide undergoes a bathochromic shift comparable to L-Trp in solution. However, at pH 13, the peptide adopts a conformation in which Trp appears to be less exposed to the solvent (bathochromic shift of only 1.0 nm compared with 1.5 nm for L-Trp, Table 2). Bathochromic shifts for Trp in both the sonicated DNA−peptide and the unsonicated DNA−peptide complex indicate that Trp is bound in a polar environment. The dialysis-induced binding produces a complex in which Trp is in a less polar environment judged by its smaller bathochromic shift.

Table 2: 0,0-Emission Band vs Excitation Wavelength of the Tryptophan in the Central Domain of Bull Protamine at 77 K

sample/% EG	λ_{exc} (nm)[a]	λ_{em} (nm)[b]	bathochromic shift (nm)
L-Trp[c]	285		
	300		1.5
peptide/H_2O/30% (pH 7)	280	407.8	
	295	409.2	1.4
peptide/H_2O/30% (pH 13)	280	407.9	
	295	408.9	1.0
CT-DNA/peptide (dialysis method)	280	411.7	
	295	412.1	0.4
CT-DNA/peptide (sonicated DNA)	285	411.1	
	295	412.5	1.4
CT-DNA/peptide (unsonicated DNA)	280	409.0	
	295	412.6	3.6[d]

[a] Samples were excited at two different wavelengths using 16 nm band-pass. [b] The 0,0-band emission was recorded using 3 nm band-pass. [c] Reference 37. [d] Very broad 0,0-band, difficult to measure accurately.

Slow-Passage ODMR. The zero field splitting (zfs) parameters are given in Table 3. The peptide produces ODMR transitions at 1.74 and 2.52 GHz for the $D - E$ and $2E$ transitions, respectively; the $D + E$ transition is absent; this pattern is normally observed for unperturbed Trp (*24*, *25*). The values for the zfs parameters are very similar to those of free Trp. The $D - E$ transition frequency decreases by 90−120 MHz, in general, upon binding the peptide to CT DNA in all samples, while the $2E$ transition frequency undergoes relatively little change. Figure 3 shows the zero field ODMR transitions for the peptide at pH 7, the complex formed with sonicated DNA, and the poly(dABrdU)−peptide complex. We have measured the ODMR transition frequencies vs observed wavelength within the 0,0-band that reveal a linear dependence with the phosphorescence emission wavelength (data not shown). This correlation is typical of solvent exposed Trp and has been observed previously in

Table 3: ODMR Transition Frequencies and zfs Parameters of Tryptophan in Various Environments

sample[a]	λ_{em} (nm)[b]	ODMR freq (GHz)[c]			zfs parameter (GHz)	
		$D-E$	$2E$	$D+E$	D	E
L-Trp[d]	406.0	1.74 (165)	2.45 (345)		2.97	1.23
Lys-Trp-Lys[e] peptide	409.3	1.76 (147)	2.49 (276)		3.00	1.24
pH 7	408.5 ± 0.2	1.74 (110)	2.52 (195)		3.00	1.26
pH 13	409.0 ± 0.2	1.71 (99)	2.54 (137)		2.98	1.27
CT DNA + peptide sonicated DNA						
mixing method	412.4 ± 0.2	1.67	2.49		2.92	1.25
dialysis method	411.9 ± 0.2	1.64	2.59		2.93	1.29
Poly(dABrdU) + peptide	414.9 ± 0.6	1.74[f] (195)	2.72[f] (311)	4.29[f] (280)	3.01	1.36
BrdU oligomer + peptide	417.6 ± 0.1		2.70[f]	4.28[f]	2.93	1.35

[a] Samples were excited at 295 nm with 16 nm band-pass. All samples at pH 7, unless noted. [b] Emission monitored at the 0,0-band with 3 nm band-pass. Emissions with standard deviations are averages at 77, 4.2, and 1.2 K; heavy atom perturbed complexes are averages at 4.2 and 1.2 K; otherwise $T = 4.2$ K. [c] ODMR frequencies were obtained using the slow passage technique at 1.2 K; $D - E$ and $2E$ signals were corrected for fast passage effects while the $D + E$ transition was not; microwave sweep rates and conditions vary according to sample, see text. Line widths (FWHH) in parentheses, in MHz. [d] Reference 36. [e] Reference 34. [f] ODMR transitions not corrected for rapid passage effects.

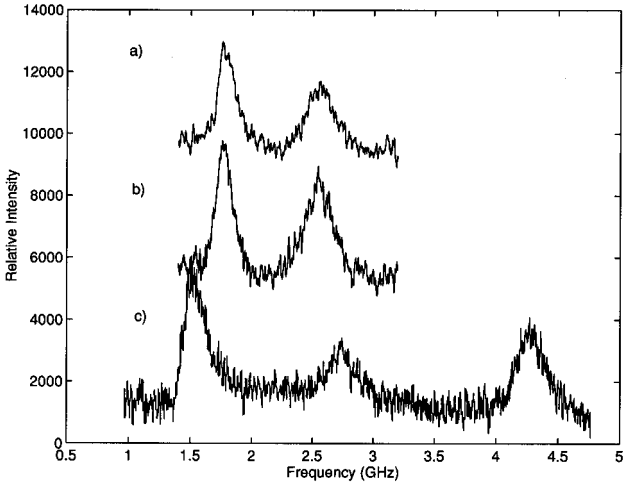

FIGURE 3: Zero-field ODMR at 1.2 K of (a) $D - E$ and $2E$ transitions for the peptide at pH 7; sweep rate of approximately 50 MHz/s, (b) $D - E$ and $2E$ transitions for sonicated DNA−peptide complex; sweep rate of approximately 50 MHz/s, (c) $D - E$, $2E$, and $D + E$ transitions for poly(dABrdU)−peptide; sweep rate of 3 GHz/s. In curves a and b, the microwaves were swept through the $D + E$ signal region (data not shown) but no ODMR signal was observed. The trp 0,0-band is monitored with 3.2 nm band-pass with excitation at 295 nm. Sample conditions are given in the Figure 1 caption.

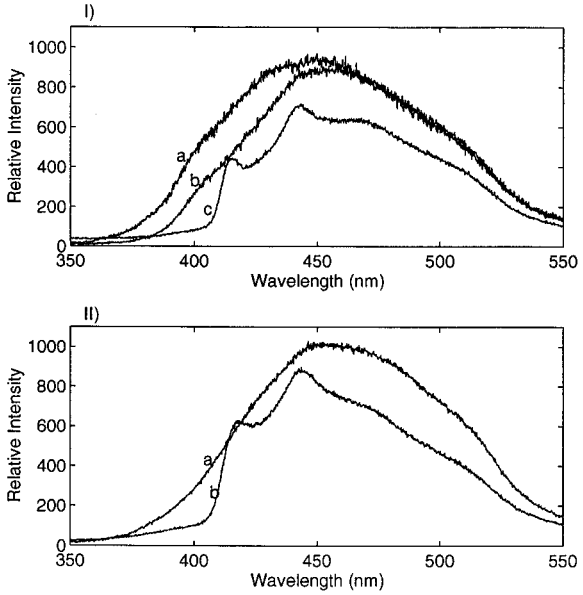

FIGURE 4: Phosphorescence spectra of brominated DNA and its complexes. (Ia) Poly(dABrdU) at 77 K with excitation at 295 nm, in solution, (Ib) same as panel Ia but with excitation at 308 nm, (Ic) Poly(dABrdU)−peptide wet solid at 4.2 K with excitation at 295 nm. (IIa) Seventeen base pair duplex oligo(dABrdU), in solution, (IIb) oligo(dABrdU)/peptide complex, wet solid; both at 4.2 K and excitation at 295 nm. Buffer is 10 mM TRIS, pH 7, containing 23% EG (v/v) in all samples.

indole and L-Trp (*31*, *32*). The wavelength dependence of the $D - E$ transition has a slope of −0.015 GHz/nm for complexes with both sonicated and unsonicated DNA and a slope of −0.012 GHz/nm for the free peptide. The similarity in slopes of the zfs vs wavelength between the peptide and the complexes points to a similar degree of local polarity in the three samples.

Sublevel Kinetics. Table 1 contains the apparent decay rate constants of the individual triplet sublevels obtained from the MIDP experiments. The k values cited for L-Trp in Table 1 have been corrected for spin-lattice relaxation (*33*), but no such corrections were performed in this study. The apparent sublevel decay constants obtained for the peptide are influenced by spin-lattice relaxation (SLR) and small variations in their values are likely to be due to the effects of SLR. The apparent k_x of Trp in the bound complex is 2.7 times larger than that in the free peptide. The average triplet state lifetime calculated from the individual sublevel ks of the sonicated DNA−peptide complex is 2.54 s, which corresponds closely to the short component (2.8 s) of the decay at 77 K. Since the microwave pulse was applied only between 6 and 12 s after shutting off the excitation, the Trp population with shortened lifetimes could have been favored in the MIDP experiment.

Heavy Atom Perturbation. The phosphorescence spectrum of poly(dABrdU) at 77 K using two different excitation wavelengths appears in Figure 4. The phosphorescence spectrum of a 17 base pair alternating dA-BrdU oligonucleotide also is shown in the same figure. The spectra are similar to those reported previously (*19*); some differences in band shape and peak wavelengths can be attributed to differences in photomuliplier and grating response, since none of these spectra were corrected for quantum efficiency effects. The triplet state of the brominated polynucleotide decays with apparent lifetime components of 950 and 180 μs, as determined at 4.2 K using Xe flash lamp excitation (*19*).

The phosphorescence of the poly(dABrdU)−peptide complex is structured, resembling that of Trp. It has the most red-shifted and least resolved phosphorescence spectrum of all the complexes. The center of the 0,0-band peaks at around 415.0 nm (Figures 1, panel f, and 4 panel Ic, Table 3). The phosphorescence decay required a triexponential model for a satisfactory fit of the data (Table 1) yielding the shorter components of 0.25 s (31%) and 0.04 s (46%), both attributed to heavy atom-perturbed Trp (*21*). These lifetimes are ca. 25 and 150 times shorter, respectively, than those of Trp in the free peptide or in its complex with calf thymus DNA (Figure 2c). A longer-lived contribution was present that is assigned to a relatively unperturbed Trp. This usually consisted of 11−24% of a 4.4−4.9 s component, which remained after washing the precipitate 2−3 times with buffer/EG mixture. The fraction of longer-lived component decreased as the phosphorescence was monitored to the red, with a concomitant increase in the shorter-lived components attributed to Trp subjected to a HAE. The relatively unperturbed Trp phosphorescence could be attributed to Trp sites that are not in sufficient contact with Br to produce a large HAE. The most prominent feature in the ODMR spectra is the appearance of the $D + E$ transition (Figure 3), confirming the HAE on Trp. The $D + E$ transition also is induced in the tripeptide, lysyl tryptophanyl lysine (Lys-Trp-Lys), when it binds to poly(dABrdU), and similar shortened phosphorescence decay components are observed (*21*). There is an increase of ca. 200 MHz in the 2E transition frequency relative to the CT DNA−peptide complex and the unbound peptide. The $D - E$ frequency, on the other hand, remains close to its value in the peptide. The fast passage transient technique (*28*) was used on the $D - E$, 2E, and $D + E$ transitions to give k_x and k_y (Table 1). Both the 2E and $D + E$ transitions gave the same value for one of the decay rate constants. This is attributed to k_y, since fast passage yields responses from only the radiative sublevels of the triplet state and the only radiative sublevel in common with these two transitions is the T_y sublevel. Fast passage through the $D - E$ transition gave k_x while MIDP measurements exciting the $D + E$ transition were used to obtain k_z. The apparent decay rate constant of the T_x sublevel in the complex is ca. 500 times its value in the peptide.

DISCUSSION

Evidence for Major Groove Binding and External Heavy Atom Effect. The appearance of the $D + E$ ODMR transition (*21, 34*), fluorescence quenching with enhanced phosphorescence yield (data not shown) (*16*), and decrease in the phosphorescence lifetimes (*25*) were all documented in the poly(dABrdU)−peptide complexes. Each of these effects is considered diagnostic of a heavy atom perturbation and require Trp to be very close to (approximating van der Waals contact with) the Br atom. This is only possible if the peptide binds in the major groove of DNA, the location of the Br atom. The red shift relative to the other complexes and the broadening of the 0,0-band can be attributed to the highly polarizable environment produced by bromine. The peptide binding to the major groove of DNA, with the side chain of Trp directed inward toward the DNA core, agrees with results for the DNA−peptide complexes discussed below. Although the ODMR transitions were not corrected for rapid passage effects, it is obvious that the 2E transition has increased in frequency with respect to all the other samples. The interaction between Br and indole could involve the edge of the ring. Br, with its large, highly polarizable electronic cloud, could possibly interact with the $\partial(+)$ edge and bring about the increase observed in the 2E transition frequency. The order of magnitude of the HAE to be expected from Br atom perturbation is given by the phosphorescence decay kinetics of indole incorporated into the dibromobenzene lattice, in which it is in van der Waals contact with Br atoms (*35*). The two distinctly oriented indoles decay with phosphorescence lifetimes of 12 and 33 ms, respectively. Thus, the decay kinetics observed for the peptide−poly(dABrdU) complex (Table 1) are consistent with a Br-induced HAE. Maki and Cha (*21*), in their study of Lys-Trp-Lys binding to poly(dABrdU), argued that Trp could only lie within the major groove of DNA with its ring parallel to the stacked bases, since unstacking of the bases (which was not observed) would occur otherwise. It was suggested that the HAE on Trp occurred as a result of partial intercalation of Trp.

Trp Microenvironment in the Peptide. The peptide in solution displays a solvent exposed Trp with 0,0-band at 408.5 ± 0.2 nm, line width of 11.4 ± 0.7 nm, bathochromic shifts upon exciting to the red of the absorption band, and D and E values close to those of L-Trp in solution (Tables 1−3). However, the 0,0-band is red shifted from that of L-Trp by 2.5 nm (*36*), suggesting a more polarizable environment; the hydrophobic portions of the arginine side chain appear to contribute to the environment experienced by Trp.

The width of the 0,0-band reveals the degree of randomness of the intermolecular interactions between a chromophore and its immediate environment that are trapped in the glass (*26*). The more polar the microenvironment of Trp the stronger are the dipole−dipole interactions and the greater is the heterogeneity displayed. The peptide 0,0-band is somewhat broader than that of L-Trp in solution. The presence of hydrophobic R side chains in addition to polar solvent molecules is probably the reason for the increased heterogeneity. In general, 0,0-bands with wavelengths ≤410 nm originate from polar sites, while those at wavelengths ≥410 nm are associated with less polar, more polarizable environments (*32*). On the basis of this criterion, the peptide/solvent system provides a solvent exposed micro environment for Trp.

The bathochromic shift, which is most apparent in polar solvents (*26*), turns out to be an effective experiment (*37*) to determine the degree of solvent exposure in proteins. A smaller bathochromic shift is found for Trp in the peptide at pH 13 than for L-Trp and the peptide at pH 7. This provides evidence that Trp is in a less polar environment at pH 13 than at pH 7. The lack of tertiary conformation in a peptide this size precludes the observation of a large pH effect such as the large wavelength shifts associated with denaturation/renaturation that are recorded in larger proteins (*38*). Neutralization of the R side chains at pH 13 probably allows the Trp to condense into a less polar environment. However, heterogeneity of the microenvironment does not increase greatly based on 0,0-band widths (Table 1).

Analysis of the peptide by computer modeling with energy minimization (*10*) portrays only one R side chain in the vicinity of the indole ring of Trp at any time. Solution NMR (^{13}C T_1 relaxation measurements) of R_6WGR_6 (*39*) suggest a large mobility for the epsilon carbon of R in comparison

with backbone carbons. When a solution is cooled to form a glass at 1.2 K, these rotational and vibrational motions are effectively eliminated. However, a range of structures are trapped in the glass as evidenced by the broad line widths that characterize phosphorescence and ODMR measurements on solvent exposed trps. The variability among individual samples in the position of the 0,0-band peak wavelength also provides evidence of the flexibility of the peptide before binding (*37*). This effect was observed in the peptide at pH 7, which displayed variability in the 0,0-band of the same sample from day to day.

Trp Microenvironments in DNA Complexes. The CT DNA−peptide complexes show 0,0-bands that are broader than those of the peptide in solution at pH 7 (Figure 1, Table 1) suggesting that an increase in the local heterogeneity occurs upon complex formation. The broadest and least resolved 0,0-band among those observed occurs in the complex with unsonicated DNA. Since direct mixing was used, the binding occurs very rapidly, with immediate formation of a precipitate. A solution of unsonicated DNA is viscous and the fact that the binding occurs so rapidly suggests that not all the potential binding sites are exposed evenly or remain available for binding to the peptide. Hence, the peptide binds in a less uniform fashion exposing the Trp to a greater variety of environments. The larger heterogeneity around Trp will translate into a broader 0,0-band. The complex formed by gradient dialysis shows the best resolved and narrowest 0,0-band of all measured complexes with CT DNA. In this case, the DNA was sonicated prior to mixing, and since the salt concentration is slowly decreased by dialysis, the actual binding should occur in a more ordered fashion. A precipitate is not observed immediately as with the mixing methods, but is only observed after cooling. A finer precipitate is formed, due to the smaller fragments of DNA. That the dialysis binding actually produced a DNA−peptide complex, instead of aggregated peptide which (although unlikely) also could precipitate, is demonstrated by (1) the degree of phosphorescence red shift (Table 3) exhibited by the sample and (2) a smaller bathochromic shift (Table 2) suggesting a more hydrophobic environment.

The phosphorescence red shift in the 0,0-band (Table 3) upon binding to CT DNA suggests that the Trp is now found in a more polarizable environment. The $D - E$ transition decreases by 90−120 MHz upon binding, while the $2E$ transition is relatively unaffected. The decrease in the frequency of the $D - E$ transition is often associated with increased polarizability of a Trp site in a protein (*32*). However, this is usually associated with an increase in E, with D remaining relatively unaffected (*32*). In the case of peptide binding to CT DNA, however, the D parameter is reduced with E being relatively unchanged (Table 3). This pattern is characteristic of the effect of aromatic stacking interactions which reduce D specifically, because of charge transfer effects. Such effects are particularly evident in the triplet states of aromatic phanes (*40*, *41*) which exhibit both a reduction of D as well as a phosphorescence red shift as the result of stacking. The reduction of D found in the peptide−CT DNA complexes (3−4%) is not as large as in some examples of Trp stacking, where it can approach 10%, as in the complexing of *Escherichia coli* single-stranded DNA binding protein with poly(dT) (*42*). Stacking of Trp with DNA bases was also found to decrease the phosphorescence lifetime, specifically by enhancement of k_x (*42*). The pattern of zfs changes and phosphorescence red shift observed in this work suggests that partial stacking with DNA bases, rather than a more general hydrophobic effect is responsible. Stacking effects also may be associated with the decreased phosphorescence lifetime (by enhancement of k_x) of a Trp population in the CT DNA complexes.

The zfs parameters are very similar among the complexes prepared by different methods. However, the bathochromic shifts (Table 2) for complexes prepared by the mixing method suggest greater local polarity than for the complex formed by dialysis. The suggestion of a polarizable environment along with solvent polar interactions for Trp in the two former CT DNA complexes appears contradictory. Binding to DNA probably brings Trp closer to the ionic interaction region of the phosphate oxygens and the positive charges of R, especially once bound in a complex where movement of the peptide is restricted. In fact, ab initio calculations have suggested stabilizing interactions between the amino groups of Lys and Arg, among others, and the aromatic rings of Phe, Tyr, and Trp (*43*, *44*). Since the edges of the aromatic rings are $\partial(+)$ and the π electrons of the ring are $\partial(-)$, the amino−aromatic interaction should occur with the π electronic cloud preferentially. Our results seem to agree with the idea that Trp directed toward the major groove could indeed be affected by the ionic binding sites, as well as interacting with the hydrophobic environment of the DNA bases. This would explain the bathochromic shift results concurrent with an increase in the polarizability of the environment as suggested by the red shift in the 0,0-band and the decrease in the frequency of the $D - E$ transition. Previous work with Lys-Trp-Lys bound to double-stranded poly(dABrdU) (*21*) reached the conclusion that the Trp was only partially stacked with the bases since lysine binding to the phosphates restricted the extent of Trp insertion into the major groove. This view of the interaction is in agreement with our interpretation of the DNA binding of the protamine analog.

The spine of hydration in DNA, first identified in a Dickerson dodecamer (*45*), lies in the minor groove in the AT region. This has been classified as type I bound water, or ordered water by NMR standards, which remains bound to protons in the minor groove for a time longer than required for molecular tumbling (*46*). The kinetics of DNA hydration appear to be salt dependent, with type I water entering the type II regime at higher ionic strength. Protons that interact with type II bound water are independent of ionic strength denoting that they have very loosely associated water molecules. This is the type of water that has been found associated with the major groove of DNA (*46*). Therefore, the possibility of Trp in contact with water in the major groove is not totally excluded.

Our results point to the existence of two populations of Trp in these peptide−DNA complexes. One population of Trp is directed into the major groove of DNA such that its decay from an excited state is affected by the Br present in BrdU, while another population does not interact with the bases of DNA. This would be supported by the decay data presented in Table I. The contribution of the shorter lifetime component of ∼2−3 s increases while that of the longer lived component of ∼6.5 s decreases as the phosphorescence of the complex is monitored further to the red. The former represents the population that is perturbed by stacking interactions with the DNA bases. This population of Trp

must all point into the major groove of the DNA to which they are complexed and not into a nearby DNA. The distance between helical axes of adjacent DNA molecules complexed with protamine has been estimated to be 26 Å by X-ray diffraction (*4*). Modeling of the complexes (*9*) suggests that protamine fits inside the major groove and extends only slightly beyond the confines of the DNA molecule. A complexed peptide with Trp sticking out of the major groove would not extend far enough toward neighboring DNA helices to interact with their bases (or Br) if the two helices are separated by this distance (26 Å). Although our results demonstrate that the peptide binds to the major groove of DNA, we cannot rule out the possiblity of other types of interactions, since an unperturbed Trp population is usually present in our samples. These include minor groove binding, the possibility of Trp sticking out of the major groove but not into other DNAs, and the possibility that not all Trp in peptides complexed to the major groove are within van der Waals distance of a Br atom.

Conclusions. The peptide R_6WGR_6, a model of the central binding domain of bull protamine, binds to the major groove of double-stranded poly(dABrdU), a conclusion which also can be extended to CT DNA binding. Bound Trp showed effects that could only be explained if it is directed into the major groove environment of double-stranded DNA; the phosphorescence and ODMR results on peptide−CT DNA complexes are consistent with a binding model in which Trp is partially stacked with nucleobases. Our results suggest that bull protamine, containing three regions of six contiguous arginines in its binding domain, binds in the same fashion, with the native aromatic side chain, phenylalanine, directed into the major groove of DNA.

ACKNOWLEDGMENT

We would like to thank Joseph Mazrimas and Shelley Corzett for helpful discussions and general laboratory assistance.

REFERENCES

1. Phillips, D. M. (1974) *Spermiogenesis*, Academic Press, Inc., New York.
2. Balhorn, R. (1989) in *Molecular Biology of Chromosome Function* (Adolph, K. E., Ed.) pp 366−395, Springer-Verlag, New York.
3. Pogany, G. C., Corzett, M., Weston, S., and Balhorn, R. (1981) *Exp. Cell. Res. 136*, 127−136.
4. Puigjaner, L. C., Fita, I., Arnott, S., Chandrasekaran, R., and Subirana, J. A. (1986) *J. Biomol. Struct. Dyn. 3*, 1067−1078.
5. Campos, J. L., Subirana, J. A., Aymami, J., Mayer, R., Giralt, E., and Pedroso, E. (1980) *Stud. Biophys. 81*, 3−14.
6. Warrant, R. W., and Kim, S.-H. (1978) *Nature 271*, 130−135.
7. Balhorn, R. (1982) *J. Cell Biol. 93*, 298−305.
8. Bradbury, E. M., Prince, W. C., and Wilkinson, G. R. (1962) *J. Mol. Biol. 4*, 39−49.
9. Hud, N. V., Milanovich, F. P., and Balhorn, R. (1994) *Biochemistry 33*, 7528−7535.
10. Hud, N. V. (1992) Ph.D. Thesis, University of California, Davis, CA.
11. Darynkiewicz, Z., Gledhill, B. L., and Ringertz, N. R. (1969) *Exp. Cell Res. 58*, 435−438.
12. Balhorn, R., Kellaris, K., Corzett, M., and Clancy, C. (1985) *Gamete Res. 12*, 411−422.
13. Vicars, L. J. (1990) M. S. Thesis, San Jose State University, San Jose, CA.
14. Kasha, M. (1952) *J. Chem. Phys. 20*, 71.
15. McGlynn, S. P., Azumi, T., and Kinoshita, M. (1969) *Molecular Spectroscopy of the Triplet State*, Prentice-Hall, Englewood Cliffs, N. J.
16. Galley, W. C., and Purkey, R. M. (1972) *Proc. Natl. Acad. Sci. 69*, 2198−2202.
17. Anderson, R. R., Maki, A. H., and Ott, C. M. (1980) *Biochemistry 19*, 4412−4418.
18. Cha, T. A., and Maki, A. H. (1982) *Biochemistry 24*, 6586−6590.
19. Cha, T.-A., and Maki, A. H. (1984) *Biochim. Biophys. Acta 799*, 171−180.
20. Hélène, C., Toulmé, J., and Le Doan, T. (1979) *Nucleic Acids Res. 7*, 1945.
21. Maki, A. H., and Cha, T. (1983) in *Photochemistry and Photobiology*, Proc. Int. Conf., Univ. of Alexandria, Egypt (Zewail, A. H., Ed.) pp 1035−1055, Harwood, Chur.
22. Hershberger, M. W., and Maki, A. H. (1980) *Biopolymers 19*, 1329−1344.
23. Hoff, A. J. (1989) in *Advanced EPR. Applications in Biology and Biochemistry* (Hoff, A. J., Ed.) pp 633−684, Elsevier, Amsterdam.
24. Maki, A. H. (1984) in *Biological Magnetic Resonance*, vol. 6 (Berliner, L. J., and Reuben, J., Eds.) pp 187−294, Plenum Press, New York.
25. Maki, A. H. (1995) *Methods Enzymol. 246*, 610−638.
26. Galley, W. C., and Purkey, R. M. (1970) *Proc. Natl. Acad. Sci. 67*, 1116−1121.
27. Schmidt, J., Veeman, W. S., and van der Waals, J. H. (1969) *Chem. Phys. Lett. 4*, 341−345.
28. Winscom, C. J., and Maki, A. H. (1971) *Chem. Phys. Lett. 12*, 264−268.
29. Lamola, A. A., Gueron, M., Yamane, T., Eisinger, J., and Schulman R. G. (1967) *J. Chem. Phys. 47*, 2210−2217.
30. Dinse, K. P., and Maki, A. H. (1976) *Chem. Phys. Lett. 38*, 125−129.
31. von Schütz, J. U., Zuclich, J., and Maki, A. H. (1974) *J. Am. Chem. Soc. 96*, 714−718.
32. Kwiram, A. L. (1982) in *Triplet State ODMR Spectroscopy* (Clarke, R. H., Ed.) pp 427−478, Wiley-Interscience, New York.
33. Ozarowki, A., Wu, J. Q., and Maki, A. H. (1996) *J. Magn. Reson., Ser. A 121*, 178−186.
34. Khamis, M. I., Casas-Finet, J. R., and Maki, A. H. (1987) *J. Biol. Chem. 262*, 1725−1733.
35. Smith, C. A., and Maki, A. H. (1993) *J. Phys. Chem. 97*, 997−1003.
36. Zuclich, J., Schweitzer, D., and Maki, A. H. (1973) *Photochem. Photobiol. 18*, 161−168.
37. Schlyer, B. D. (1991) Ph.D. Thesis, University of California, Davis, CA.
38. Demchenko, A. P. (1986) *Ultraviolet Spectroscopy of Proteins*, Springer-Verlag, Germany.
39. Prieto, M. C. (1997) Ph.D. Thesis, University of California, Davis, CA.
40. Schweitzer, D., Colpa, J. P., Behnke, J., Hausser, K. H., Haenel, M., and Staab, H. S. (1975) *Chem. Phys. 11*, 373−384.
41. Haenel, M. W., and Schweitzer, D. (1988) *Adv. Chem. Ser. 217*, 333−355.
42. Tsao, D. H. H., Casas-Finet, J. R., Maki, A. H., and Chase, J. W. (1989) *Biophys. J. 55*, 927−936.
43. Burley, S. K., and Petsko, G. A. (1985) *Science 229*, 23−28.
44. Burley, S. K., and Petsko, G. A. (1986) *FEBS Lett. 203*, 139−143.
45. Kopka, M. L., Fratini, A. V., Drew, H. R., and Dickerson, R. E. (1983) *J. Mol. Biol. 163*, 129.
46. Kubinec, M. G., and Wemmer, D. E. (1992) *J. Am. Chem. Soc., 114*, 8739−8740.

BI971061L